Article

Removal of Transition-Metal Ions by Metal-Complexing Polythiosemicarbazone Membranes

Roman Nickisch, Wiebe M. de Vos, Michael A. R. Meier, and Muhammad Irshad Baig*

Cite This: *ACS Appl. Polym. Mater.* 2023, 5, 7240–7251

Read Online

ACCESS | Metrics & More | Article Recommendations | Supporting Information

ABSTRACT: Membrane technology is one of the many strategies to remove transition-metal ions from aqueous streams because of its relatively lower costs and ease of operation. Typically, adsorbent materials are added into polymeric membranes to impart chelating/complexing properties, but this often results in a limited number of adsorption sites within the membrane. In this work, polythiosemicarbazone (pTSC) is proposed as a material to prepare polymeric membranes due to its metal-complexing ligands in the backbone, providing more adsorption sites. The polymer was easily processed into membranes via the nonsolvent-induced phase separation technique and exhibited asymmetric structures with adequate mechanical strength. The porosity of the membranes was controlled by increasing the polymer concentration in the casting solution, leading to ultrafiltration- and nanofiltration-type membranes with permeabilities ranging from 30 to 0.7 L·m^{-2}·h^{-1}·bar^{-1}. The resulting pTSC membranes were applied for the removal of silver and copper ions in batch and, in the case of silver ions, also in dynamic adsorption experiments. The maximum removal rate of 17 mg·g^{-1} for silver and 3.8 mg·g^{-1} for copper ions was obtained in the batch removal experiment. Streaming potential, pH measurements, and infrared spectroscopy (FTIR) were conducted to verify the anionic binding of TSC groups, while neutral binding modes were revealed by FTIR and batch removal experiments. Furthermore, the removal of silver ions was also successfully demonstrated in a flow setup operated at 4 bar of applied pressure. The streaming potential and energy-dispersive X-ray (EDX) spectroscopy conducted on the membranes after the flow tests confirmed the complexation by TSC-functional groups as the separation mechanism. Finally, partial desorption of the silver ions was successfully conducted in water to demonstrate the reusability of pTSC membranes.

KEYWORDS: chelating polymer, metal–polymer complex, membrane, adsorption, ultrafiltration, transition-metal ions
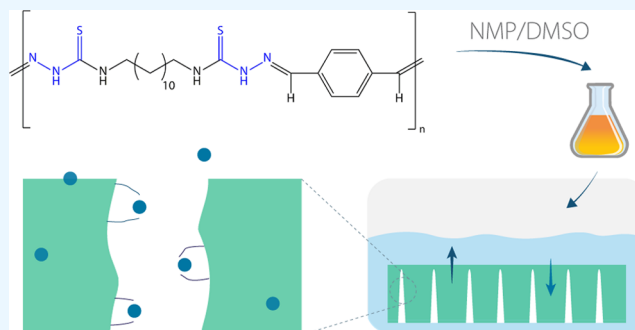
1. INTRODUCTION

Heavy metal ions are well-known pollutants in aqueous streams and often end up in groundwater sources around the world.[1] Typical examples are arsenic, lead, mercury, nickel, copper, silver, and chromium. The major contributors of such pollutant ions are the mining and metal processing industries, especially in the developing world, where effective legislation and its implementation are still lacking. These ions can be toxic (e.g., carcinogenic), thus posing a serious health hazard to humans and aquatic life.[2] The removal of such ions from aqueous streams is essential for a safer and cleaner environment. From a different perspective, recovering these pollutants can also lead to sustainable development in the sense of urban mining.[3]

Several techniques are in place to effectively remove heavy metal ions from aqueous streams such as adsorption,[4] precipitation/coagulation,[5] electrochemical treatments,[6] and membrane-based filtration.[7] Each technique has its advantages and limitations. For instance, chemical precipitation provides a high d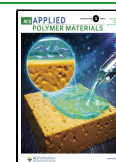egree of selectivity but typically requires large amounts of precipitation agents, which creates a difficulty in disposing of sludge.[8] Electrochemical treatment requires electric power and is mostly effective at lower ionic concentrations. Adsorption is a simple technique, where a wide variety of absorbers can be used to target heavy metal ions. It has the advantage of having fast adsorption kinetics and high metal uptake capacity.[9] However, the adsorbent must have sufficient chemical stability against regenerating agents.

Membrane-based heavy metal ion removal is a one-step approach that has emerged as one of the options. Typically, the membranes used for ions/salt removal have lower water fluxes and generally separate ions via a combination of different mechanisms like Donnan exclusion, dielectric exclusion, or
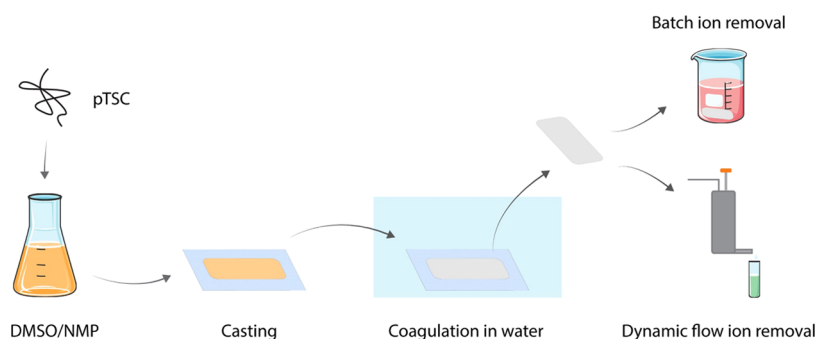
solution diffusion.[10] Samavati et al. reviewed several commercially available nanofiltration membranes that can effectively remove heavy metal ions such as nickel, chromium, copper, lead, zinc, and cobalt.[11] Similarly, other types of membrane materials like mixed matrix membranes and nanofibers have also been investigated for ion removal and water treatment by several researchers.[12−15] In addition to the lower water fluxes, the nanofiltration membranes are often prone to scaling due to the presence of other multivalent salts in the aqueous feed streams. A pretreatment step is therefore sometimes needed to reduce fouling and scaling on the membrane surface, resulting in higher-energy demand and increased costs. Therefore, combining the membrane filtration with an adsorption approach can be advantageous because an adsorptive membrane separates the metal ions via specific interactions like complexation/chelation, e.g., by hydrogen-bonding and $\pi-\pi$ interactions that exist between the functional groups of the membranes and the heavy metal ions.[16] Consequently, adsorptive membranes have the advantage of maintaining higher water fluxes while essentially retaining heavy metal ion selectivity.[17] Vo et al. summarized many different types of adsorptive membranes in their review and highlighted their versatility in terms of regeneration and reusability.[18]

Typically, adsorptive membranes are prepared by adding adsorbents into the polymer membranes using different modification strategies such as blending, grafting, or coating.[19] Chelate-forming groups have been integrated into different types of membrane matrices using these techniques for the removal of heavy metal ions.[20−23] However, such membranes have limited specific surface area and a lower number of adsorption sites that are available for the adsorbent−metal interactions. As a result, the overall adsorption capacity of the membranes is low, meaning that they can only process low concentrations of heavy metal ions. Although this limitation has somewhat been addressed by incorporating nanomaterials like metal−organic frameworks (MOFs)[24] or graphene oxide,[25] which has led to the significantly improved adsorption capacity of the mixed matrix membranes, the limited stability of MOFs in alkaline or acidic conditions hinders their regeneration and operation in the long term.[16]

By preparing polymeric membranes having metal chelating/complexing groups in the polymer backbone, the adsorption sites and the adsorption capacity can be significantly enhanced, as each monomer unit provides at least one adsorption site. Preparing an adsorptive membrane with such a polymer has the advantage of being a simple and scalable approach. In this regard, chitosan and its blend membranes have been widely investigated for complexing metal ions due to the presence of amino and hydroxyl groups, where the lone pair of O and N atoms is responsible for adsorption.[26] Reiad et al. prepared a chitosan/polyethylene glycol blend membrane with adsorption capacities of up to 38 mg·g^{-1} for iron and 18 mg·g^{-1} for manganese having a 98% desorption efficiency.[27] Similarly, Ghaee et al. prepared cross-linked chitosan membranes using silica gel as a pore-forming agent, obtaining 19.9 mg·g^{-1} of copper ion and 5.2 mg·g^{-1} of nickel ion adsorption.[28] However, a major limitation of chitosan membranes is their solubility in acid and lower mechanical strength. Membranes made from other polymers have also been reported in the literature for the removal of transition-metal ions. For instance, Denizli et al. investigated the polymer poly(2-hydroxyethyl methacrylate-methacryloylamidohistidine) as a membrane

material for the adsorption of cadmium, lead, and mercury and reported adsorptions of 8.2, 31.5, and 23.2 mg·g^{-1}, respectively.[29] Similarly, Villalobos et al. fabricated poly-thiosemicarbazide membranes for the recovery of gold and reported a significantly high adsorption of ~1 g·g^{-1}.[30] These membranes also exhibited acid stability having desorption ratios >97% coupled with enhanced mechanical stability. Only a limited amount of literature is available on such types of metal-complexing polymers, mainly because it is difficult to fabricate mechanically strong membranes out of them.

In this work, we propose polythiosemicarbazone (pTSC) as a metal-complexing polymer to fabricate membranes for transition-metal ion removal from aqueous streams. The structure of the investigated pTSC polymer is depicted in Figure 1, which contains two complexing thiosemicarbazone

Figure 1. Chemical structure of the polythiosemicarbazone (pTSC) polymer used for membrane preparation by NIPS, depicting the typical complexing functional group in blue.

(TSC) ligands per repeat unit that forms complexes with transition-metal ions.[31−34] Herein, we use the recently introduced pTSCs obtained by feasible polycondensation of dithiosemicarbazones and dialdehydes[34,35] to prepare poly-meric pTSC membranes for the first time and demonstrate their transition ion removal performance. The polymer was first dissolved in either dimethyl sulfoxide (DMSO) or 1-methyl-2-pyrrolidinone (NMP) to obtain casting solutions, which were transformed into solid membranes by immersion in a water bath. The resulting membranes were characterized in terms of their morphologies, water permeabilities, ion removal performance, and mechanical and pH stability. The resulting membranes showed decent silver and copper metal ion removal while demonstrating good mechanical and pH stability.

2. MATERIALS AND METHODS

2.1. Materials. The chemicals dimethyl sulfoxide (DMSO, ≥99.9%, ACS reagent), 1-methyl-2-pyrrolidinone (NMP, ≥99.9%, ACS reagent), poly(ethylene glycol) (molecular weights 200, 400, 600, 1000, 1500, 2000 Da), MgCl$_2$ (≥98%, anhydrous), MgSO$_4$ (≥99.5%, anhydrous, ReagentPlus), Na$_2$SO$_4$ (≥99.0%, anhydrous, granular, ACS reagent), NaCl (≥99.0%, ACS reagent), AgNO$_3$ (99.99%), ZnCl$_2$ (≥98%, reagent grade), CuCl$_2$·2H$_2$O (99%), glycerol solution (≥99.5%, ACS reagent), bovine serum albumin (BSA, ≥96%, lyophilized powder), sodium phosphate monobasic dihydrate (≥99.0%), and sodium phosphate dibasic heptahydrate (≥99.99%) were purchased from Merck, The Netherlands. Deionized water was obtained from Milli-Q Benchtop Lab Water Purification Systems. All of the chemicals were used as received.

2.2. Synthesis of pTSC Polymer. The polymer polythiosemi-carbazone (pTSC) was synthesized according to the protocol mentioned in our earlier work.[34] Briefly, N,N′-(dodecane-1,12-diyl) bis(hydrazinecarbothioamide) (1.00 g, 2.87 mol, 1.00 equiv) and terephthaldehyde (385 mg, 2.87 mmol, 1.00 equiv) were added to 1.9 mL of DMSO and the reaction was stirred at room temperature for 2 h. Subsequently, 2 mL of NMP was added to the reaction mixture to solubilize the polymer using a sonification bath (50 °C, 80 kHz).

Figure 2. Schematic illustration of the experimental procedure followed to fabricate and characterize pTSC membranes for transition-metal ion removal.

Precipitation was performed by the dropwise addition of the polymer solution to 400 mL of cold water. The polymer was filtered, suspended in 400 mL of water, refluxed for 1 h, and subsequently cooled and filtered to remove DMSO and NMP. This process was repeated three times. The polymer was obtained after drying at 100 °C and 12 mbar for at least 20 h. The pTSC product was obtained as yellow polymer balls (1.25 g) in a yield of 98% containing less than 1 wt % DMSO.[34]

2.3. Membrane Fabrication and Characterization. The pTSC polymer was dissolved in DMSO or NMP in different concentrations (7−20 wt %) at room temperature. The resulting polymer solution was cast on a glass plate using a casting bar having a gap height of 400 μm. The cast film was immediately immersed in a deionized water (20 °C) bath resulting in the precipitation of the polymer and subsequent formation of a membrane. Regardless of the polymer concentration, all of the membranes precipitated within 1.5 s. The membranes were taken out of the bath and were washed three times with water to remove any remaining solvent. A schematic illustration of the experimental procedure to obtain pTSC membranes is depicted in Figure 2.

A scanning electron microscope (SEM, JSM-6010LA, JEOL, Japan) equipped with energy-dispersive X-ray spectroscopy (EDS) was used to take images of the membranes. The membrane samples were first coated with a 5 nm layer of Pt/Pd (80/20) alloy using a Quorum Q150T ES (Quorum Technologies, Ltd., U.K.) sputter coating machine. For cross-sectional SEM imaging, the membrane samples were immersed in liquid nitrogen for 20 s and immediately fractured to reveal the cross section. The average pore size of the separation layer was estimated from the top surface SEM images of the membranes by analyzing the images using an in-house-developed Python code. The program first converts the grayscale SEM image to a binary image by thresholding and then identifies the edges of completely dark areas (pores) in the membrane matrix. The maximum lengths of these paths were then calculated based on the "maximum ferret length" built-in function. This provides the lengths of all of the pores of the image, which were then plotted in a histogram having a bin size of 25 nm. The histogram was converted into a scatter plot with pore (bin) sizes on the *x*-axis and frequency (%) of pores on the y-axis. The plot was finally fitted via the log−normal distribution function to reveal the pore size distribution and the average pore size (nm). It is important to note that the pore size distribution obtained in this manner is not precise but provides an estimate for comparison purposes.

Fourier-transformed infrared spectroscopy (FTIR) was performed on a Spectrum Two (PerkinElmer) in the wavenumber range of 4000−600 cm^{-1}. The water contact angle of the membranes was measured on an OCA 20 (Data Physics Instruments GmbH, Germany) using a sessile drop (3 μL) technique. The contact angle was measured via the built-in software 5 s after the droplet had made contact with the membrane surface.

For the pure water permeability (PWP) measurements, the membranes were cut into a 25 mm circular disk and mounted on a dead-end Amicon cell setup, which utilized nitrogen gas to pressurize the water. All of the permeability tests were conducted at a pressure of 3 bar. The mass of the permeating water was measured as a function of time via an electronic weighing balance connected to a computer. The pure water permeability (PWP) P was calculated using eq 1

$$ P = \frac{J}{\Delta p} = \frac{V}{A \times t \times \Delta p} \tag{1} $$

where J is the pure water flux, V is the volume of water (L), A is the membrane area (m^2), t is the time (h), and Δp is the pressure difference (bar) between the feed and permeate side.

The pH stability of the membranes was evaluated by immersing the membrane pieces in 0.1 M HCl (pH 1) and 1 M NaOH (pH 14) for 7 days. Subsequently, the membrane pieces were taken out, washed with deionized water three times, and tested for their PWP. A comparison of PWP values of untreated and pH-treated membranes indicated the membrane's pH stability.

The retention of different types of salts was conducted by filtering a 5 mM aqueous solution of either NaCl, Na$_2$SO$_4$, MgSO$_4$, or MgCl$_2$ through the membranes in a dead-end configuration with continuous stirring. The conductivity of the salt solutions with known concentrations was first measured using a handheld conductivity meter WTW Cond 3210 (Xylem Analytics, Germany), and a calibration curve was plotted. The concentrations of the salt in the feed, permeate, and retentate were then calculated based on the calibration curve. Retention R (%) was calculated using eq 2

$$ R = \left[1 - \frac{C_p}{C_f + C_r} \right] \tag{2} $$

where C_p, C_f, and C_r are the concentrations of salt in the permeate, feed, and retentate, respectively.

The molecular weight cutoff (MWCO) of the membranes was determined by filtering a solution containing PEGs having different molecular weights, i.e., 200, 400, 600, 1000, 1500, 2000, and 4000 Da, each at a concentration of 1 g·L^{-1}. The feed, permeate, and retentate were analyzed using gel permeation chromatography (GPC, Agilent 1200/1260 Infinity GPC/SEC series, Polymer Standards Service data center, and column compartment). An aqueous solution of 50 mg·L^{-1} NaN$_3$ was used as the eluent for the GPC column, and the concentrations of PEGs were determined by the GPC via the refractive index. The retentions were calculated using eq 2 and plotted as a function of the PEG molecular weight to obtain a sieving curve. The MWCO was then determined as the molecular weight of PEG, which is 90% rejected. A 0.1 wt % BSA solution prepared in 0.1 M phosphate buffer at pH 7.4 was used to evaluate the ultrafiltration performance of the membranes. The permeation test was conducted in a dead-end cell with constant stirring at a feed pressure of 1 bar. The feed, permeate, and retentate samples were collected, and the respective concentrations were analyzed using a UV−vis spectrophotometer (Shimadzu UV-1800, Japan) at an absorbance wavelength of 280 nm. The retention was calculated using eq 2.

2.4. Ion Removal Experiments. The removal of three metals from the respective salts, i.e., AgNO$_3$, ZnCl$_2$, and CuCl$_2$, was
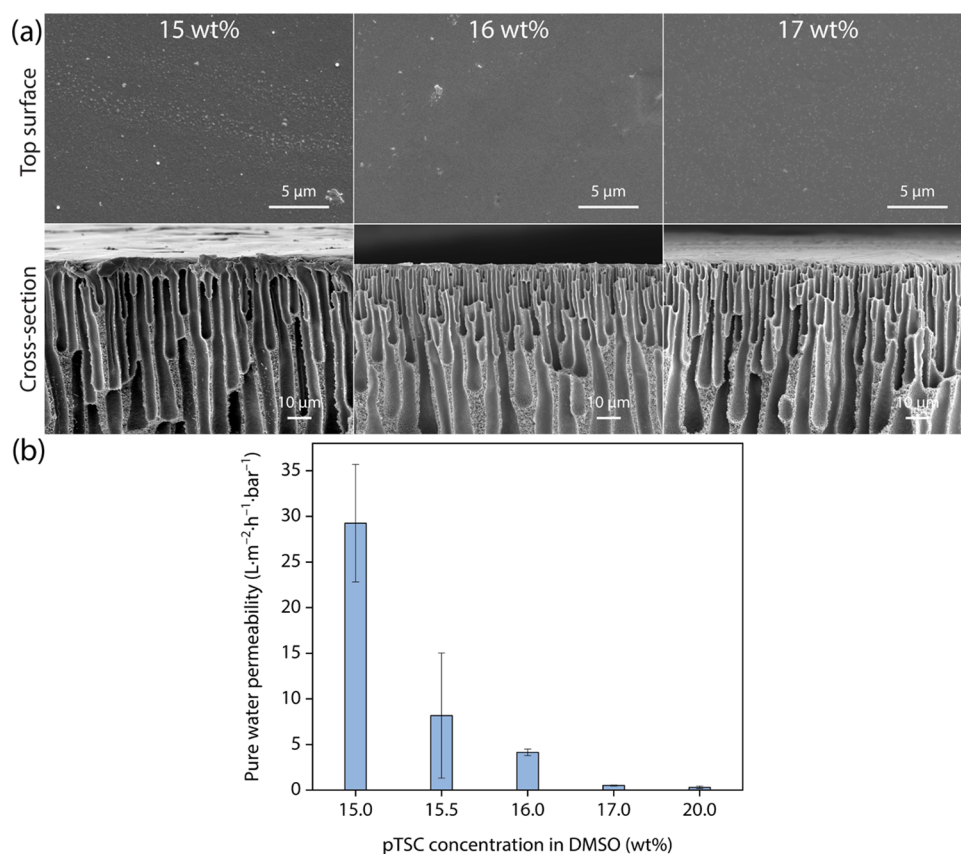
Figure 3. (a) Top surface and cross-sectional SEM images and (b) pure water permeability (PWP) of the pTSC membranes prepared using DMSO as a solvent. Membranes were prepared using 15−20 wt % of pTSC in DMSO. The PWP tests were conducted at a feed water pressure of 3 bar.

evaluated via two methods (see Figure 2 for the schematic illustration). The first one was the batch removal experiment where an 8 cm^2 (20 cm^2 for AgNO$_3$) membrane piece was immersed in a 5 mL (16 mL for AgNO$_3$) aqueous solution of 1.25 mM salts for 5 days (1, 6, 24, 120 h for AgNO$_3$) under continuous shaking. The ion concentration of the salt solution before and after immersion was determined via ion chromatography (IC) on an 858 Professional Sample Processor, a 2× Eco IC, Metrohm (Switzerland), consisting of an anion column (Metrosep A Supp 17-150/4.0) and a cation column (Metrosep C 6-150/4.0). An aqueous solution of 4 mM HNO$_3$ (0.6 mL·min^{-1}) and 5 mM Na$_2$CO$_3$ (0.9 mL·min^{-1}) was used as an eluent for cation and anion columns, respectively. The ion removal rate (r, %) and the ion removal per unit mass (g) of the membrane (r_m, mg·g^{-1}) were calculated using eqs 3a and 3b, respectively

$$r = \left(1 - \frac{C_t}{C_f}\right) \times 100 \tag{3a}$$

$$r_m = \left(\frac{r \times n \times A_m}{m}\right) \tag{3b}$$

where C_t and C_f are the concentrations of the respective ions of the sample after a certain time (t) and the concentration of ions in the feed solution, respectively. In eq 3b, n is the overall amount (millimoles) of the respective ion applied, A_m is the atomic mass of the cation (g·mol^{-1}), and m is the mass of the membrane piece used (g).

In the second method, the removal of AgNO$_3$ was investigated in a dynamic flow (Amicon cell) setup as a proof of concept. A 20 mL aqueous solution of AgNO$_3$ (1.25 mM) was filtered through the 3.8 cm^2 membrane in a dead-end configuration. After the test, the membranes were taken out and analyzed using EDS and streaming potential (SurPASS electrokinetic analyzer, Anton Paar, Graz, Austria).

2.5. Complexation Reaction of pTSC with Salts. The polymer pTSC (50 mg, corresponding to ∼224 μmol TSC groups) was dissolved in 1.12 mL of DMSO. Afterward, AgNO$_3$ or CuCl$_2$·2H$_2$O (19.0 μg, 112 μmol) was added and the mixture was stirred at 80 °C for 80 min. Subsequently, 1.12 mL of DMSO was added to the suspension and further stirred at 80 °C for 2 h. Then, 2.24 mL of DMSO was added and the reaction was again stirred at 80 °C for 19 h. The reaction mixture was cooled to room temperature, and the formed precipitate was filtered off. Finally, the obtained brown solid was washed with water and dried at 80 °C overnight.

3. RESULTS AND DISCUSSION

3.1. Morphology and Pure Water Permeability. Two sets of pTSC membranes were prepared in this work. For the first set, DMSO was used as a solvent, and for the second set, NMP was used. The prepared pTSC solutions were cast as thin films on glass plates and immediately immersed in a nonsolvent water bath, where precipitation occurred within 1.5 s.

Figure 3a shows the SEM images of the resulting membranes obtained using DMSO as the solvent. All of the membranes possessed a dense top surface with no visible pores at a given magnification of ×5000. The cross section of the membranes exhibited a typical asymmetric morphology having a denser top layer followed by well-defined finger-like macrovoids in the substructure. The existence of such macrovoids is a characteristic indication of the instantaneous phase separation and a rapid rate of polymer precipitation.[36,37] Furthermore, there was no significant change in the membrane morphology upon increasing the polymer concentration from 15 to 20 wt % (see Figure S1 for SEM images). It must be noted that lower pTSC
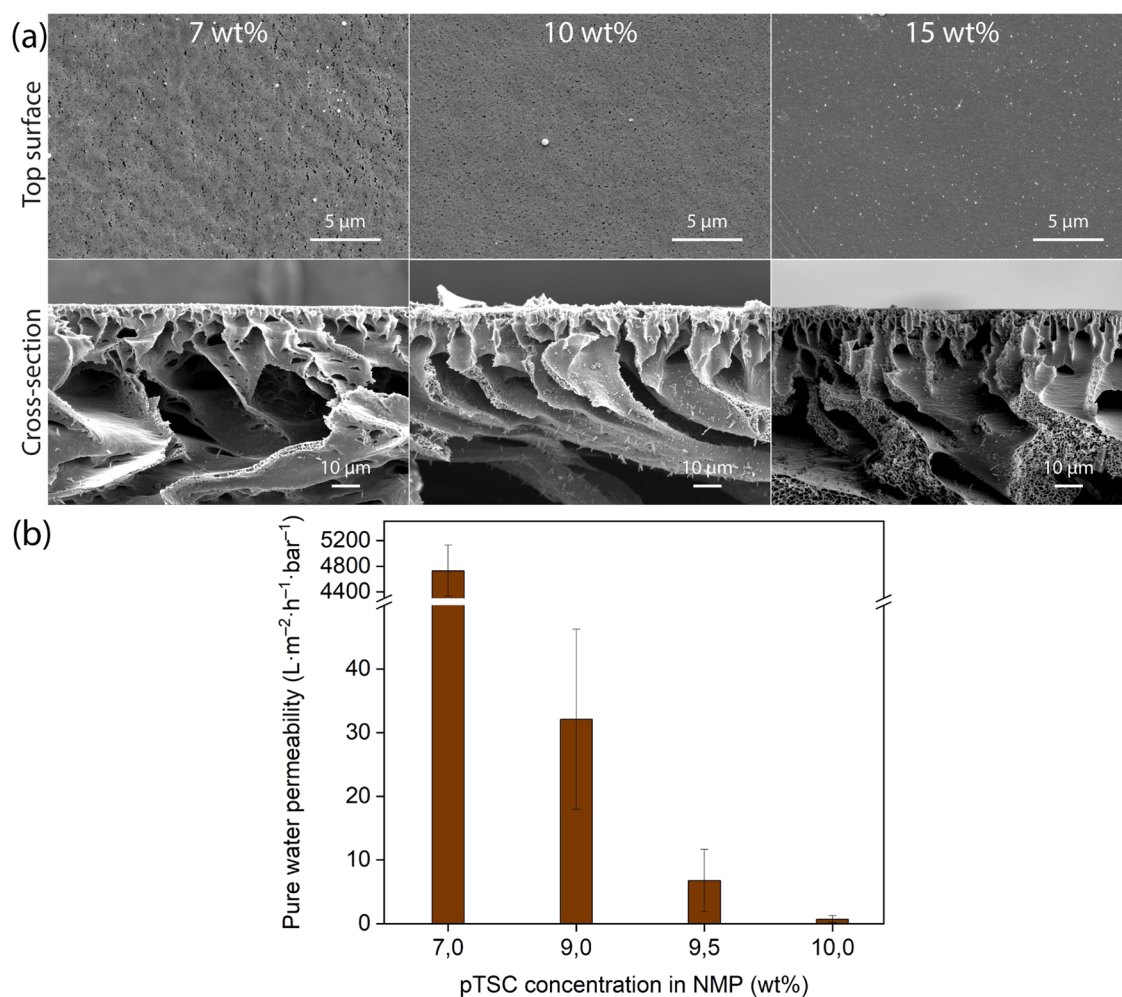
Figure 4. (a) Top surface and cross-sectional SEM images and (b) pure water permeability (PWP) of the pTSC membranes prepared using NMP as a solvent. Membranes were prepared using 7−15 wt % pTSC in NMP. The PWP tests were conducted at a feed water pressure of 3 bar.

concentrations in DMSO such as 5−10 wt % resulted in brittle membranes that could not be processed further.

However, the pure water permeability (PWP) of the membranes significantly decreased with increasing polymer concentration (see Figure 3b). At a 15 wt % pTSC concentration, the resulting membranes had a PWP of ~29 ± 6 $L \cdot m^{-2} \cdot h^{-1} \cdot bar^{-1}$. Increasing the polymer concentration to 16 wt % resulted in a significant drop in the PWP value to ~4 ± 0.3 $L \cdot m^{-2} \cdot h^{-1} \cdot bar^{-1}$. As the polymer concentration in the casting solution was further increased to 20 wt %, the PWP dropped to ~0.3 $L \cdot m^{-2} \cdot h^{-1} \cdot bar^{-1}$. Although the SEM images reveal no significant change in the membrane morphology at the given magnification, the PWP indicates that increasing the polymer concentration leads to a denser membrane structure. This effect is well studied in the published literature, and it has been reported that a higher polymer concentration in the casting solution leads to more polymer at the binodal phase separation point in the ternary phase diagram, ultimately leading to a compact membrane structure.[36,37]

Based on the PWP values alone, the 15 wt % pTSC membranes can be categorized as tight ultrafiltration (UF), while the rest as nanofiltration (NF)-type membranes. To establish a separation performance, aqueous solutions of 0.1 wt % BSA or 5 mM salts (NaCl, Na_2SO_4, $MgSO_4$, or $MgCl_2$) were filtered through the membranes in a dead-end configuration.

The 15 wt % pTSC membrane showed complete retention of BSA without any retention of salts. BSA has a molecular weight of ~66.5 kDa and a hydrodynamic diameter (D_h) of ~7 nm.[38] The retention results indicate that the membrane separates BSA according to the size-exclusion mechanism, meaning that the pores of the membrane are significantly smaller than 7 nm, the D_h of BSA. On the other hand, no retention of salts indicates that the membrane is not a nanofiltration type. Consequently, the membrane could effectively be used for UF applications, such as concentrating protein solutions, while allowing the salts to pass through.

Similarly, and as expected, the 16 wt % pTSC membranes also completely retained BSA though without any salt retentions. Having a PWP of ~4 $L \cdot m^{-2} \cdot h^{-1} \cdot bar^{-1}$, which is in the range of typical NF membranes, it was expected that the membrane may retain multivalent salts. The membrane surface charge, measured via streaming potential, was approximately −38 mV. This result was reasonable because the pTSC group exhibits an acidic proton attached to the hydrazide moiety of the TSC group (the chemical shift of the respective proton in a ^{1}H NMR spectrum in DMSO-d_6 was 11.50 ppm).[34] A clear connection between the pK_a value of TSCs and their deep-field signal of the NH-hydrazide proton has been reported by Mendes et al.[39] The negative charge would mean that the membrane can retain co-ions via the Donnan exclusion
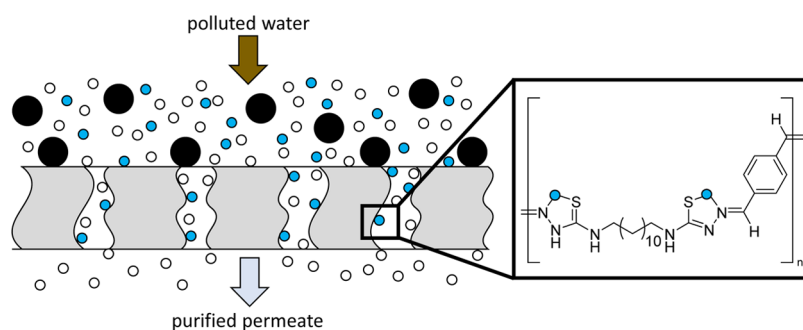
Figure 5. Envisioned water purification using the pTSC membrane. Besides size separation (depicted by the larger black spheres not being able to pass through the membrane), complexation allows the removal of transition metals (blue spheres) as well, which would otherwise pass through due to their small size. In addition, the complexation of the metal ions by the TSC groups is schematically shown by a neutral and anionic complexation on the right.

mechanism, resulting in higher retentions for Na_2SO_4. However, that was not the case and no retentions were found for any of the salts tested ($NaCl$, Na_2SO_4, and $MgCl_2$). Next, the MWCO of the membrane, which can provide more information about the estimated pore diameter of the membranes, was determined. A sieving curve, shown in Figure S2, was recorded, leading to an MWCO of approximately 2300 Da. This value is significantly higher compared to NF-type membranes, which typically have MWCOs in the range of (200−1000 Da) with pore diameters generally smaller than 2 nm.[10,40] The average molecular weight (M) of PEG has been correlated to its Stokes diameter d_s (nm) using eq 4[41−43]

$$d_s = 33.46 \times 10^{-3} \times M^{0.557} \tag{4}$$

For a PEG M_w of 2300 Da, the Stokes diameter is ~2.5 nm. Consequently, it is estimated that the 16 wt % pTSC membrane, having an MWCO of 2300, has an average pore diameter slightly larger than 2.5 nm. The MWCO coupled with the estimated average pore diameter results explains why the membrane did not retain any salt. The physical stability of the 16 wt % pTSC membranes was evaluated by conducting a PWP test at 4 bar of water pressure for 7 days. The results presented in Figure S3 show that the membranes maintain their permeability of ~4 $L \cdot m^{-2} \cdot h^{-1} \cdot bar^{-1}$ for the entire duration of the test. Similarly, the pH stability of the membranes was evaluated by immersing different pieces of the same membrane in pH 1 and 14 solutions for 7 days. The PWP did not change significantly (Figure S4) even after exposure to extreme pH values, demonstrating the stability of pTSC membranes against strong acid (HCl) and base (NaOH). The 17 and 20 wt % pTSC membranes were not tested further for their separation performance because of their low permeabilities of <0.5 $L \cdot m^{-2} \cdot h^{-1} \cdot bar^{-1}$, which makes their use impractical.

Figures 4a and S1 depict the SEM images of the pTSC membranes when NMP was used as a solvent. A 5 wt % pTSC membrane was also prepared but did not possess adequate mechanical strength for further processing. It is evident from the top surface SEM images that the surface becomes denser upon increasing the polymer concentration from 7 to 20 wt %. At polymer concentrations of 7 and 10 wt %, there are visible pores on the membrane surface. The average pore diameter of the membranes, estimated using SEM image analysis, was ~80 and ~66 nm for 7 and 10 wt % pTSC membranes, respectively. The pore size distribution of the membranes is shown in Figure S5. The 7 wt % pTSC membranes have a large pore size

distribution ranging to ~700 nm. In comparison, the pore diameter of 10 wt % pTSC membrane did not exceed 350 nm. These results are expected because, as explained before, the membranes become denser as the polymer concentration in the casting solution is increased. Further increasing the polymer concentration to 15 wt % and then to 20 wt % resulted in membranes that did not show any visible pores at the shown magnification of ×5000. The SEM images of the 20 wt % pTSC membranes are shown in Figure S1. In addition, the cross-sectional SEM images reveal that all of the membranes had an asymmetric structure having a relatively compact top layer with finger-like macrovoids in the substructure. The major difference between the three cross-sectional SEM images shown in Figure 4a is that the substructure also densifies with the increase in polymer concentration from 7 to 15 wt %.

The PWP of the resulting membranes is shown in Figure 4b. In accordance with the membrane structure, the PWP of the membranes decreases remarkably when the polymer concentration is increased. At a concentration of 7 wt % pTSC in NMP, the PWP of the resulting membranes was about 4700 ± 400 $L \cdot m^{-2} \cdot h^{-1} \cdot bar^{-1}$, which decreased to about 32 ± 14 $L \cdot m^{-2} \cdot h^{-1} \cdot bar^{-1}$ when the polymer concentration is increased to 9 wt %. Further increasing the polymer concentration to 9.5 wt % and then to 10 wt % led to significantly lower PWP values of 6 ± 4.5 and 0.7 ± 0.5 $L \cdot m^{-2} \cdot h^{-1} \cdot bar^{-1}$, respectively. Membranes obtained from a polymer solution in NMP with a weight percentage of the polymer higher than 10 resulted in dense membranes exhibiting no PWP at all. It was found that using NMP as a solvent led to considerable deviations in PWP values even for the same polymer concentration (larger error bars in comparison to DMSO-derived membranes). This was assumed to be a result of the rapid precipitation during the NIPS process while using NMP as a solvent that was, compared to DMSO, even faster, which was assigned to a higher miscibility of NMP with water as compared to DMSO.[44] Additionally, it was found that pTSC showed a slightly higher solubility in NMP as compared to that of DMSO. This was observed by preparing 20 wt % of pTSC solutions in each solvent and storing them for 3 months. The solution prepared in DMSO became cloudy after 1 month, which could be transformed into a clear solution again by stirring it under heating at ~50 °C. On the other hand, no change was observed for the pTSC in NMP solution even after 3 months. Furthermore, the membranes prepared using NMP as a solvent exhibited stable

Table 1. Removal Rates of ZnCl$_2$, CuCl$_2$·2H$_2$O, and AgNO$_3$ Solutions by pTSC Membranes Measured by Ion Chromatography (IC)

salt	cation-removal (%)	anion-removal (%)	cation-removal, r_m (mg·g^{-1})	active TSC group (%)[a]
ZnCl$_2$	5	0	1	0.3
CuCl$_2$·2H$_2$O	23	4	3.8	1.3
AgNO$_3$	53	24	17	3.0

[a]The value was determined by dividing the amount of the removed metal cation by the amount of used TSC-functional groups assuming successful complexation is obtained with one TSC group per metal ion.
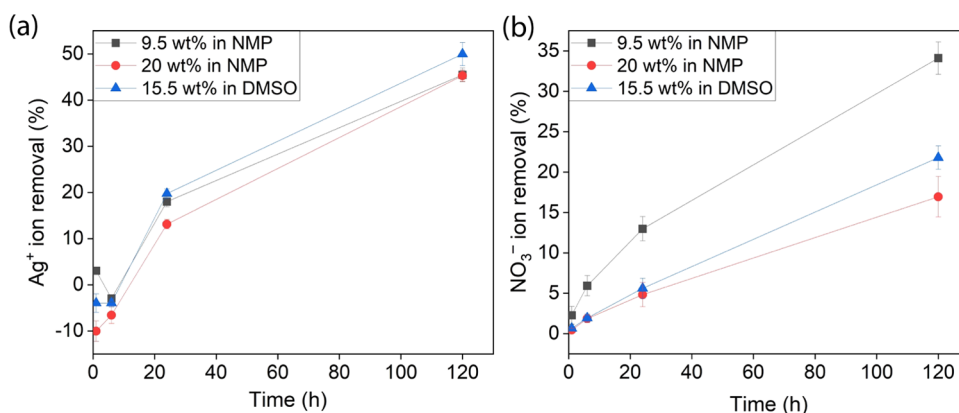
Figure 6. Batch adsorption kinetics of silver and nitrate ions. The pTSC membranes were prepared using different concentrations of polymer in either NMP or DMSO. A 20 cm^2 piece of the respective membrane was immersed in 20 mL of 1.25 mM AgNO$_3$ solution, and the concentrations of ions were measured as a function of time.

PWP values after 7 days of exposure to pH 1 and 14 solutions, demonstrating their pH stability.

3.2. Removal of Transition-Metal Ions. The removal of salts from water streams is usually carried out via reverse osmosis (RO) or NF membranes using a separation mechanism that is often a combination of the Donnan exclusion, dielectric exclusion, and steric hindrance. Moreover, these membranes have significantly lower water fluxes than MF- and UF-type membranes. Comparatively, the removal of salts by complexation can be carried out at higher water fluxes. For instance, water permeabilities of 180−467 L·m^{-2}·h^{-1}·bar^{-1} with the quantitative removal of metals have been reported in the literature.[30,45] Additionally, it is challenging to find a suitable polymer capable of sufficient complexation with metals, while delivering mechanical stability to allow application in a membrane process.[30]

The TSC group exhibits in general a strong affinity to several transition-metal ions like Cu, Zn, Au, Hg, and Ni via several different anionic and neutral binding modes.[33] These complexation reactions have been reported to take place at room temperatures for several examples such as Zn, Pd, Pt, and Ag.[46−48] Furthermore, similar functional groups, like thioureas and thiosemicarbazides, are known to remove metal ions like Au or Hg with high sensitivities and selectivities from aqueous solutions.[30,49] Thus, it was envisioned to use the obtained pTSC membranes for the removal of transition-metal ions from an aqueous solution. Figure 5 shows the schematic representation of the complexation-based metal ion removal from aqueous streams by the pTSC membranes.

3.2.1. Batch Removal Experiments. In a first batch removal experiment, 8 cm^2 of pTSC membrane made from a 9.5 wt % polymer solution in NMP was immersed in 5 mL of an aqueous solution of 1.25 mM of the salts ZnCl$_2$, CuCl$_2$·2H$_2$O, and AgNO$_3$ (i.e., overall amount of salt 6.25 μmol). A membrane area of 8 cm^2 was approximately equal to 25 mg of

membrane material and thus depicted a considerable excess of functional groups, which could potentially bind the metal ions. The used salts were chosen as suitable test substrates according to the above-discussed literature data, and the membrane was immersed in the solution for 5 days under shaking. Subsequently, a sample was taken from the solution and the ion concentration was determined by IC. The ion removal rates (%), calculated using eqs 3a and 3b, are summarized in Table 1.

Nearly no removal of zinc was obtained, while copper ions were removed to an extent of 23%. The highest removal rate of 53% was obtained for silver ions, which, according to eq 3b, amounts to 17 mg of silver ions removed per gram of the membrane by complexation of 3% of the available TSC-functional groups. Since not all TSC groups present in the membrane are accessible for the metal ions, it can be expected that the percentage of the TSC groups available for complexation is small. Similar values have been reported in the literature for membranes applied for metal removal. For instance, Villalobos et al. reported the application of poly-(thiosemicarbazide)s for the removal of copper and gold ions, showing that 1.7 and 15% of the active groups removed cations, respectively.[30] These percentages were calculated using the given data reported by the authors of the manuscript.[30] Since the highest removal rate was obtained for AgNO$_3$ in this work, the kinetics of the batch adsorption experiment was monitored for membranes (20 cm^2) made from polymer casting solutions with different weight percentages of polymer using DMSO or NMP as solvent (see Figure 6). The corresponding mass was 72 mg for 9.5 wt % in NMP, 146 mg for 20 wt % in NMP, and 131 mg for 15.5 wt % in the DMSO membrane.

Comparing the membranes obtained using different solvents and polymer concentrations, the different membrane morphologies seemed to have a minor impact on the overall
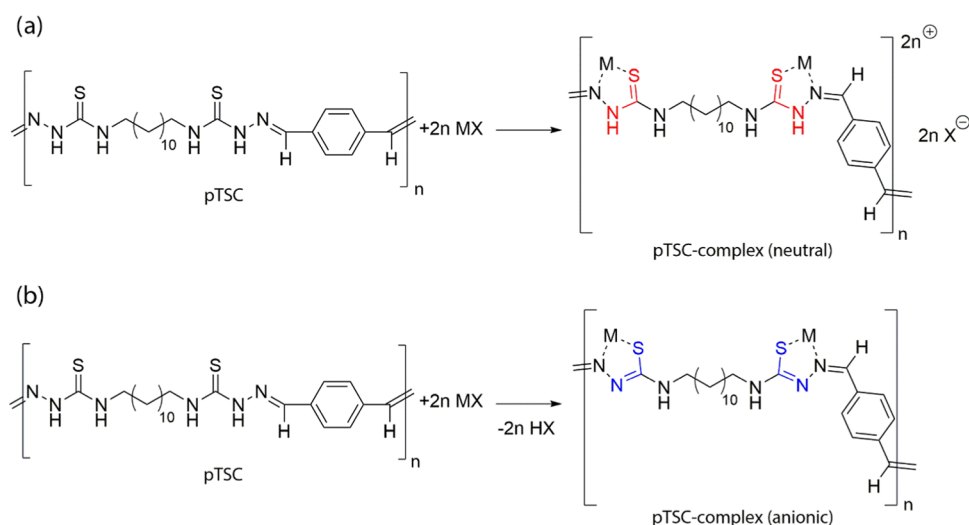
Figure 7. Schematic overview of the (a) neutral (red) and (b) anionic (blue) complexation of a metal salt (MX) by pTSC.

removal rate for the silver ions. This finding supports a complexation-type removal mechanism. Compared to the first batch adsorption experiment, the membrane obtained from a 9.5 wt % polymer in NMP yielded a more pronounced removal (r_m) of the anion, i.e., 7.3 mg·g^{-1} as compared to 20 wt % in NMP and 15.5 wt % in DMSO membranes, which only removed the anions at a rate of 1.8 and 2.6 mg·g^{-1}, respectively. The membranes prepared at higher pTSC concentrations had more mass, which explains their low metal removal per mass of the membrane. The complexation rate of the silver ions was comparable over time. For instance, after 1 day, the membrane made from 9.5 wt % of polymer solution in NMP reached a removal rate for silver ions of 18% (6.7 mg·g^{-1}). Still, by comparing the removal rates of silver ions for smaller time frames, it can be seen that a certain error margin is present for the experiment, i.e., negative values obtained after 1 and 6 h. This was because the IC analysis was performed at the lower resolution limit of the respective ion concentrations. The resolution limit for the respective salt was determined by measuring samples with concentrations 5, 2.5, 1.25, 0.625, and 0.313 mM on the IC. The evaluation showed that the linear dependency of the integral values of the chromatography signal and the concentration was maintained for a concentration of 1.25 mM or higher. Nonetheless, the 9.5 wt % pTSC membranes showed the highest silver ion removal (r_m) of 17 mg·g^{-1} after 120 h. In comparison, the heavier membranes such as 15.5 wt % of pTSC in NMP and 20 wt % in NMP showed lower silver ion removal of 10.3 and 8.4 mg·g^{-1}, respectively, even though the membrane area was the same. For more detailed investigations of the kinetics of the ion removal, different analyses like inductively coupled plasma optical emission spectroscopy could be applied. Nevertheless, a clear trend can be obtained in the batch removal experiment analyzed by IC, verifying metal ions that exhibit a high complexation affinity for TSC groups.

Comparing the obtained results of the batch removal experiments, metal ions and their counterions were not removed in the same ratio as seen from the data in Table 1. For instance, whereas silver ions were removed by 53% after 5 days using a membrane made from 9.5 wt % of polymer casting solution in NMP, the NO$_3^-$ ion was only removed by 24% (see Table 1). This difference indicated the presence of anionic and neutral binding of the metal ion as schematically shown in

Figure 7. A neutral complexation also leads to the stoichiometric removal of the NO$_3^-$ ion, since charge neutrality has to be maintained, while an anionic TSC group substitutes the NO$_3^-$ ion under the release of nitric acid.

Since the streaming potential of the pTSC membrane revealed a negative surface charge, the presence of an anionic binding mode seemed reasonable. Furthermore, anionic binding should lead to a pH drop of the aqueous solution since an acid is released. Indeed, a decrease of the pH value from pH 6 (corresponds to the pH value of Milli-Q water) to approximately pH 3.5 for the batch removal of AgNO$_3$ and CuCl$_2$·2H$_2$O was observed. This assumption was further underpinned by the reaction of pTSC with AgNO$_3$, ZnCl$_2$, and CuCl$_2$·2H$_2$O in DMSO. The resulting insoluble metallopolymer complexes were analyzed by IR spectroscopy, depicting typical vibrational bonds for neutral and anionic TSC complexation (see Figure 8).

The typical strong ν (C=N) vibration of the pTSC at 1535 cm^{-1} has clearly declined, indicating a complexation via the imine functional group. Furthermore, the remaining NH$_2$ end groups of the unreacted thiosemicarbazide functional groups have also likely complexed with the metals since the δ (NH$_2$) vibration at 1630 cm^{-1} has shifted toward higher wave numbers (1673 and 1667 cm^{-1}, respectively). In addition, vibrations arising due to participation of the C=S bond at 1229, 1098, and 830 cm^{-1} have shifted or declined. First, the vibration at 1229 cm^{-1} shifted to 1265 cm^{-1} for the silver metallopolymer, while it declined in the case of copper. Second, the vibration at 1098 cm^{-1} shifted in both cases to lower wave numbers (1039 cm^{-1} for the silver and 1042 cm^{-1} for the copper metallopolymer) depicting strong intensities. Lastly, the vibration at 830 cm^{-1} shifted slightly to 840 cm^{-1} for the silver and to 834 cm^{-1} for the copper. According to the literature, anionic metal−TSC complexes show a lower C=S vibrational bond at 745−820 cm^{-1} and are missing one ν(N−H) vibrational bond at 3260−3500 cm^{-1} compared to neutral complexes exhibiting a C=S vibrational bond at 800−850 cm^{-1} that is usually insignificantly shifted compared to the noncomplexed TSC compound.[33,39,50] For the obtained complex, no clear difference in the N−H region could be determined, while the C=S vibrational bond indicated neutral bonding. Additionally, bonds emerged for the silver polymer at 766 cm^{-1} and for the copper polymer at 767 cm^{-1} that could
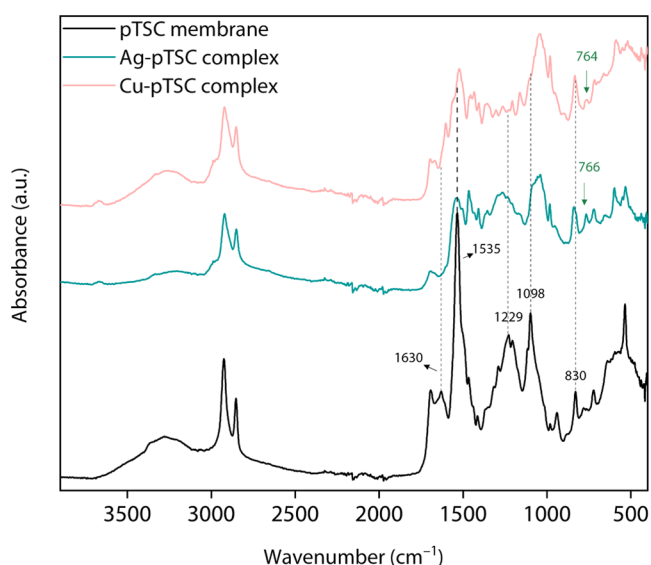
Figure 8. FTIR spectra of the pTSC membrane, Ag–TSC complex, and Cu–TSC complex membranes. Typical vibrations of the pTSC are highlighted with the respective wave numbers, while vibrations of the C=S bond indicating anionic bonding are depicted as well in green.

be related to the C=S vibrational bond of an anionic TSC–metal complex.

3.2.2. Dynamic Adsorption Experiments. In the next step, the removal of $AgNO_3$ was investigated in a dynamic flow setup as a proof of concept. Therefore, the same dead-end Amicon cell setup used for the determination of the water permeabilities of the membranes was used. Thus, 20 mL of a 1.25 mM $AgNO_3$ aqueous solution was filtered through a pTSC membrane of 3.8 cm^2 made from a 16 wt % polymer solution in DMSO. The permeability of the membrane remained the same, i.e., ~4 L·m^{-2}·h^{-1}·bar^{-1}, throughout the experiment. Successfully, the removal of silver ions could already be seen by visual observation, as the yellow membrane turned darker on the surface, while the bottom side remained yellow (see Figure S6). The removed percentage of silver ions was too low to be detected by IC due to the mentioned resolution limit. Therefore, EDX and streaming potential analysis were chosen as suitable methods to determine the content of silver ions after the conclusion of the experiments.

Due to the complexation of the cations by the TSC group, it was expected that the surface charge of the membrane would be less negative after the filtration. Indeed, a reduced negative charge of −22.9 mV was obtained for a membrane cast by using a 15 wt % polymer solution in DMSO. In comparison, the bare membrane had a negative charge of −37.8 mV. Similarly, the immersion of a membrane made from a 16 wt %

polymer in DMSO in an aqueous $AgNO_3$ solution (17.9 mM) for 2 days yielded a similarly reduced negative charge of −24.2 mV, indicating that the contact time in the flow experiment allowed sufficient complexation of the silver ions.

The EDX data summarized in Table S1 clearly show the presence of silver ions throughout the membrane (8−14 wt % of silver ions). This was expected since the top layer of an asymmetric membrane is the separation layer, and metal ions that pass this layer will also pass the more porous substructure and form complexes with the membrane material. For further comparison, the membrane prepared using 16 wt % of polymer in DMSO solution, which was later immersed in a 17.9 mM $AgNO_3$ solution for 2 days, depicted a higher amount of bound silver ions of 33−36 wt %. The EDX spectra and the respective SEM pictures are presented in Figures S8−S11.

As the removal of silver ions was successful, a desorption experiment was performed to complement this proof of concept. The desorption of the complexed silver ions is crucial for a reasonable application of the pTSC membranes for the removal of silver ions from a water stream, allowing their repetitive utilization. Thus, a membrane obtained using a 15 wt % polymer solution in DMSO was exposed to a 1.25 mM $AgNO_3$ solution in a dead-end Amicon cell setup and subsequently put in ca. 5 mL of water for 7 days. During this time, the water was exchanged three times, and afterward, the amount of silver ions was determined by EDX analysis (see Table S1). The top layer still depicted the presence of silver, while the bottom layer and the CS depicted no remaining silver. Thus, the desorption of the complexed silver ions could be partly performed by immersion in water. It seemed reasonable that the desorption rate of the substructure was higher than the top layer since the more open morphology allows easier access to water by diffusion, while the dense top layer is more restricting.

Lastly, a pTSC-$AgNO_3$ membrane was fabricated by NIPS using 15 and 16 wt % of polymer in DMSO and an aqueous solution of $AgNO_3$ (17.9 mM) as the nonsolvent (see Figure S7 for photographs of the membranes). It was expected that the resulting membranes will bear a higher charge density on the surface (presence of anionic TSC groups and the metal counterion) that could result in an improved retention of salts by the Donnan exclusion. Furthermore, silver salts often depict antimicrobial properties, which could prevent biofouling. The obtained membrane showed a different coloration (brown instead of yellow) and a surface net charge of only −10.2 mV, which was less negative than the membranes treated with $AgNO_3$ solutions (in batch or flow experiments, vide supra). This seemed reasonable since the silver ions can diffuse inside the polymer film during the precipitation process and thus can access more TSC groups in solution compared to a finished, solid membrane. However, the rigidity of the membrane

Table 2. Comparison of pTSC Membranes' Ion Removal Performance with Other Adsorbents Reported in the Literature

material	type	ions	adsorption (mg·g^{-1})	reference
clinoptilolite (zeolite)	adsorbent	silver	33.2	51
cellulose nanocrystal/nanofibers	adsorbent	silver	34.4	52
Ag$^+$-imprinted chitosan gel beads	adsorbent	silver	89.2	53
diethylenetriamine-grafted polyacrylonitrile staple fibers	adsorbent	copper	349.6	54
Fe$_3$O$_4$@polydopamine-g-L-cysteine	adsorbent	lead	46.95	55
Ce metal−organic frameworks	adsorbent	fluoride	129.7	56
polythiosemicarbazone (pTSC)	membrane/adsorbent	silver	17.7	this work

strongly increased and zero permeability was obtained after 2 days in the Amicon cell setup at 3 bar water pressure. The altered properties were assigned to the complexation of the silver ions, which could also form cross-linking by double-neutral, double-anionic, or neutral-anionic bonding of two TSC groups. Thus, the rigidity is increased and pore sizes of membranes with a certain weight percentage of polymer are decreased since the polymers are restricted in their separation during the precipitation by the cross-linking.

The pTSC polymer is shown to be an interesting candidate for making stable membranes for transition-metal ion removal. The one-step fabrication approach with embedded metal-complexing ligands is one of the major advantages of pTSC-type polymers. The silver ion removal performance of these membranes is currently lower than other adsorbents reported in the literature (see Table 2). However, further research on pTSC-based polymers can improve this aspect of the membranes.

4. CONCLUSIONS

The polythiosemicarbazone (pTSC) polymer has been successfully used to develop asymmetric membranes with tunable pore diameters and morphologies. The polymer contains complexing ligands that can effectively complex with transition-metal ions, hence helping in their removal from water streams. The pTSC membranes were produced via the nonsolvent-induced phase inversion technique by using either DMSO or NMP as a solvent. First, the membrane formation properties of pTSC were evaluated by preparing membranes from polymer solutions containing different amounts of pTSC. The polymer concentration was varied from 15 to 20 wt % in DMSO and 7 to 20 wt % in NMP. It was found that increasing the polymer concentration in both solvents led to the formation of denser membranes with water permeabilities dropping from 29 $L \cdot m^{-2} \cdot h^{-1} \cdot bar^{-1}$ for 15 wt % in DMSO to 0.3 $L \cdot m^{-2} \cdot h^{-1} \cdot bar^{-1}$ for 20 wt % of pTSC in DMSO. The 15 and 16 wt % of pTSC in DMSO membranes exhibited a high retention of BSA, with the latter membrane showing a molecular weight cutoff of around 2300 Da. These membranes could be applied for ultrafiltration applications. The membrane prepared using NMP as a solvent showed a similar performance with water permeabilities decreasing from 4700 to 0.5 $L \cdot m^{-2} \cdot h^{-1} \cdot bar^{-1}$ upon increasing the polymer concentration from 7 to 10 wt %. All of the membranes exhibited adequate mechanical strength and sustained 4 bar of applied pressure. Additionally, the membranes exhibited stable performances after exposure to 0.1 M HCl and 1 M NaOH. In the second phase, the membranes were used for silver and copper ion removal in a batch and dynamic adsorption mode. It was found that the affinity for silver was higher (3.0% active TSC groups for silver compared to 1.3% for copper). The maximum removal rate of silver by the pTSC membranes in the batch adsorption test was 17 $mg \cdot g^{-1}$ and that of copper was 3.8 $mg \cdot g^{-1}$. In addition, it was observed that the pTSC concentration during membrane preparation had a minor effect on the removal rates. Furthermore, streaming potential, FTIR, and pH tests were conducted to confirm the anionic and neutral binding of the TSC groups. The dynamic adsorption results revealed that the membrane can effectively remove transition-metal ions from water streams. The results were confirmed via streaming potential and EDX measurements where the streaming potential of the membrane became less negative, indicating the presence of complexed silver ions. On the other hand, EDX results on the membrane surface and cross section revealed the presence of silver ions, confirming the complexation of metal ions due to the complexing ligands of pTSC. Further applications of the pTSC membranes can be envisioned in the field of transition-metal ion removal from wastewater since several other metals could also exhibit affinity for this functional group.

■ ASSOCIATED CONTENT

ⓢ Supporting Information

The Supporting Information is available free of charge at https://pubs.acs.org/doi/10.1021/acsapm.3c01192.

MWCO, pore size distribution, SEM images of 20 wt % of pTSC membranes, long-term pure water permeability, pH stability, photos of membranes after adsorption of ions, and EDX analysis (PDF)

■ AUTHOR INFORMATION

Corresponding Author

Muhammad Irshad Baig − *Membrane Science and Technology Cluster, MESA+ Institute for Nanotechnology, University of Twente, Enschede 7500 AE, The Netherlands;* ⦿ orcid.org/0000-0002-7636-0630; Email: m.i.baig@utwente.nl

Authors

Roman Nickisch − *Laboratory of Applied Chemistry, Institute of Organic Chemistry (IOC), Karlsruhe Institute of Technology (KIT), 76131 Karlsruhe, Germany; Membrane Science and Technology Cluster, MESA+ Institute for Nanotechnology, University of Twente, Enschede 7500 AE, The Netherlands*

Wiebe M. de Vos − *Membrane Science and Technology Cluster, MESA+ Institute for Nanotechnology, University of Twente, Enschede 7500 AE, The Netherlands;* ⦿ orcid.org/0000-0002-0133-1931

Michael A. R. Meier − *Laboratory of Applied Chemistry, Institute of Organic Chemistry (IOC), Karlsruhe Institute of Technology (KIT), 76131 Karlsruhe, Germany; Laboratory of Applied Chemistry, Institute of Biological and Chemical Systems-Functional Molecular Systems (IBCS-FMS), Karlsruhe Institute of Technology (KIT), 76344 Eggenstein-Leopoldshafen, Germany;* ⦿ orcid.org/0000-0002-4448-5279

Complete contact information is available at:
https://pubs.acs.org/10.1021/acsapm.3c01192

Author Contributions

R.N.: conceptualization, methodology, experimentation, investigation, and writing. W.M.d.V.: project administration, supervision, writing—review and editing, and funding acquisition. M.A.R.M.: conceptualization, project administration, supervision, review and editing, and funding acquisition. M.I.B.: methodology, supervision, characterization, and writing—review and editing.

Notes

The authors declare no competing financial interest.

■ REFERENCES

(1) Saleh, T. A.; Mustaqeem, M.; Khaled, M. Water treatment technologies in removing heavy metal ions from wastewater: A review. *Environ. Nanotechnol., Monit. Manage.* **2022**, *17*, No. 100617.

(2) Dubey, S.; Shri, M.; Gupta, A.; Rani, V.; Chakrabarty, D. Toxicity and detoxification of heavy metals during plant growth and metabolism. *Environ. Chem. Lett.* **2018**, *16*, 1169−1192.

(3) Varennes, E.; Blanc, D.; Azaïs, A.; Choubert, J.-M. Upgrading wastewater treatment plants to urban mines: Are metals worth it? *Resour., Conserv. Recycl.* **2023**, *189*, No. 106738.

(4) Rajendran, S.; Priya, A. K.; Senthil Kumar, P.; Hoang, T. K. A.; Sekar, K.; Chong, K. Y.; Khoo, K. S.; Ng, H. S.; Show, P. L. A critical and recent developments on adsorption technique for removal of heavy metals from wastewater-A review. *Chemosphere* **2022**, *303*, No. 135146.

(5) Pohl, A. Removal of Heavy Metal Ions from Water and Wastewaters by Sulfur-Containing Precipitation Agents. *Water, Air, Soil Pollut.* **2020**, *231*, 503.

(6) Srimuk, P.; Su, X.; Yoon, J.; Aurbach, D.; Presser, V. Charge-transfer materials for electrochemical water desalination, ion separation and the recovery of elements. *Nat. Rev. Mater.* **2020**, *5*, 517−538.

(7) Abdullah, N.; Yusof, N.; Lau, W. J.; Jaafar, J.; Ismail, A. F. Recent trends of heavy metal removal from water/wastewater by membrane technologies. *J. Ind. Eng. Chem.* **2019**, *76*, 17−38.

(8) Wu, H.; Wang, W.; Huang, Y.; Han, G.; Yang, S.; Su, S.; Sana, H.; Peng, W.; Cao, Y.; Liu, J. Comprehensive evaluation on a prospective precipitation-flotation process for metal-ions removal from wastewater simulants. *J. Hazard. Mater.* **2019**, *371*, 592−602.

(9) Gao, X.; Guo, C.; Hao, J.; Zhao, Z.; Long, H.; Li, M. Adsorption of heavy metal ions by sodium alginate based adsorbent-a review and new perspectives. *Int. J. Biol. Macromol.* **2020**, *164*, 4423−4434.

(10) Mohammad, A. W.; Teow, Y. H.; Ang, W. L.; Chung, Y. T.; Oatley-Radcliffe, D. L.; Hilal, N. Nanofiltration membranes review: Recent advances and future prospects. *Desalination* **2015**, *356*, 226−254.

(11) Samavati, Z.; Samavati, A.; Goh, P. S.; Fauzi Ismail, A.; Sohaimi Abdullah, M. A comprehensive review of recent advances in nanofiltration membranes for heavy metal removal from wastewater. *Chem. Eng. Res. Des.* **2023**, *189*, 530−571.

(12) Wang, J.; Sun, Y.; Zhao, X.; Chen, L.; Peng, S.; Ma, C.; Duan, G.; Liu, Z.; Wang, H.; Yuan, Y.; Wang, N. A poly(amidoxime)-modified MOF macroporous membrane for high-efficient uranium extraction from seawater. *e-Polymers* **2022**, *22*, 399−410.

(13) Ma, X.; Zhao, S.; Tian, Z.; Duan, G.; Pan, H.; Yue, Y.; Li, S.; Jian, S.; Yang, W.; Liu, K.; et al. MOFs meet wood: Reusable magnetic hydrophilic composites toward efficient water reatment with super-high dye adsorption capacity at high dye concentration. *Chem. Eng. J.* **2022**, *446*, No. 136851.

(14) Jian, S.; Cheng, Y.; Ma, X.; Guo, H.; Hu, J.; Zhang, K.; Jiang, S.; Yang, W.; Duan, G. Excellent fluoride removal performance by electrospun La−Mn bimetal oxide nanofibers. *New J. Chem.* **2022**, *46*, 490−497.

(15) Jian, S.; Chen, Y.; Shi, F.; Liu, Y.; Jiang, W.; Hu, J.; Han, X.; Jiang, S.; Yang, W. Template-Free Synthesis of Magnetic La-Mn-Fe Tri-Metal Oxide Nanofibers for Efficient Fluoride Remediation: Kinetics, Isotherms, Thermodynamics and Reusability. *Polymers* **2022**, *14*, 5417.

(16) Wang, Z.; Luo, X.; Song, Z.; Lu, K.; Zhu, S.; Yang, Y.; Zhang, Y.; Fang, W.; Jin, J. Microporous polymer adsorptive membranes with high processing capacity for molecular separation. *Nat. Commun.* **2022**, *13*, No. 4169.

(17) Huang, J.; Qi, F.; Zeng, G.; Shi, L.; Li, X.; Gu, Y.; Shi, Y. Repeating recovery and reuse of SDS micelles from MEUF retentate containing Cd2 + by acidification UF. *Colloids Surf., A* **2017**, *520*, 361−368.

(18) Vo, T. S.; Hossain, M. M.; Jeong, H. M.; Kim, K. Heavy metal removal applications using adsorptive membranes. *Nano Convergence* **2020**, *7*, 36.

(19) Huang, Z.-Q.; Cheng, Z.-F. Recent advances in adsorptive membranes for removal of harmful cations. *J. Appl. Polym. Sci.* **2020**, *137*, 48579.

(20) Ibrahim, Y.; Naddeo, V.; Banat, F.; Hasan, S. W. Preparation of novel polyvinylidene fluoride (PVDF)-Tin(IV) oxide (SnO2) ion exchange mixed matrix membranes for the removal of heavy metals from aqueous solutions. *Sep. Purif. Technol.* **2020**, *250*, No. 117250.

(21) Xu, S.; Liu, Y.; Yu, Y.; Zhang, X.; Zhang, J.; Li, Y. PAN/PVDF chelating membrane for simultaneous removal of heavy metal and organic pollutants from mimic industrial wastewater. *Sep. Purif. Technol.* **2020**, *235*, No. 116185.

(22) Abdulkarem, E.; Ibrahim, Y.; Kumar, M.; Arafat, H. A.; Naddeo, V.; Banat, F.; Hasan, S. W. Polyvinylidene fluoride (PVDF)-α-zirconium phosphate (α-ZrP) nanoparticles based mixed matrix membranes for removal of heavy metal ions. *Chemosphere* **2021**, *267*, No. 128896.

(23) Dutta, M.; Jana, A.; De, S. Insights to the transport of heavy metals from an industrial effluent through functionalized bentonite incorporated mixed matrix membrane: Process modeling and analysis of the interplay of various parameters. *Chem. Eng. J.* **2021**, *413*, No. 127397.

(24) Ting, H.; Chi, H.-Y.; Lam, C. H.; Chan, K.-Y.; Kang, D.-Y. High-permeance metal−organic framework-based membrane adsorber for the removal of dye molecules in aqueous phase. *Environ. Sci.: Nano* **2017**, *4*, 2205−2214.

(25) Mukherjee, R.; Bhunia, P.; De, S. Impact of graphene oxide on removal of heavy metals using mixed matrix membrane. *Chem. Eng. J.* **2016**, *292*, 284−297.

(26) Salehi, E.; Daraei, P.; Arabi Shamsabadi, A. A review on chitosan-based adsorptive membranes. *Carbohydr. Polym.* **2016**, *152*, 419−432.

(27) Reiad, N. A.; Salam, O. E. A.; Abadir, E. F.; Harraz, F. A. Adsorptive removal of iron and manganese ions from aqueous solutions with microporous chitosan/polyethylene glycol blend membrane. *J. Environ. Sci.* **2012**, *24*, 1425−1432.

(28) Ghaee, A.; Shariaty-Niassar, M.; Barzin, J.; Zarghan, A. Adsorption of copper and nickel ions on macroporous chitosan membrane: Equilibrium study. *Appl. Surf. Sci.* **2012**, *258*, 7732−7743.

(29) Denizli, A.; Bektaş, S.; Arıca, Y.; Genç, Ö. Metal-chelating properties of poly(2-hydroxyethyl methacrylate−methacryloylamido-histidine) membranes. *J. Appl. Polym. Sci.* **2005**, *97*, 1213−1219.

(30) Villalobos, L. F.; Yapici, T.; Peinemann, K.-V. Poly-thiosemicarbazide membrane for gold recovery. *Sep. Purif. Technol.* **2014**, *136*, 94−104.

(31) Campbell, M. J. M. Transition metal complexes of thiosemicarbazide and thiosemicarbazones. *Coord. Chem. Rev.* **1975**, *15*, 279−319.

(32) Casas, J. S.; García-Tasende, M. S.; Sordo, J. Main group metal complexes of semicarbazones and thiosemicarbazones. A structural review. *Coord. Chem. Rev.* **2000**, *209*, 197−261.

(33) Lobana, T. S.; Sharma, R.; Bawa, G.; Khanna, S. Bonding and structure trends of thiosemicarbazone derivatives of metals—An overview. *Coord. Chem. Rev.* **2009**, *253*, 977−1055.

(34) Nickisch, R.; Conen, P.; Meier, M. A. R. Polythiosemicarba-zones by Condensation of Dithiosemicarbazides and Dialdehydes. *Macromolecules* **2022**, *55*, 3267−3275.

(35) Nickisch, R. Activation of Elemental Sulfur Via Multi-component Reactions for More Sustainable Organocatalysts and Sulfur-Containing Polymers, Dissertation, Karlsruher Institut für Technologie (KIT), 2023.

(36) Blanco, J.-F.; Sublet, J.; Nguyen, Q. T.; Schaetzel, P. Formation and morphology studies of different polysulfones-based membranes made by wet phase inversion process. *J. Membr. Sci.* **2006**, *283*, 27−37.

(37) Strathmann, H.; Kock, K.; Amar, P.; Baker, R. W. The formation mechanism of asymmetric membranes. *Desalination* **1975**, *16*, 179−203.

(38) Yohannes, G.; Wiedmer, S. K.; Elomaa, M.; Jussila, M.; Aseyev, V.; Riekkola, M.-L. Thermal aggregation of bovine serum albumin studied by asymmetrical flow field-flow fractionation. *Anal. Chim. Acta* **2010**, *675*, 191−198.

(39) Mendes, I. C.; Teixeira, L. R.; Lima, R.; Carneiro, T. G.; Beraldo, H. Platinum(II) complexes of 2-, 3-, and 4-formyl-pyridine thiosemicarbazone and 2-, 3- and 4-acetyl-pyridine thiosemicarbazone. *Transition Met. Chem.* **1999**, *24*, 655−658.

(40) Cao, Y.; Chen, G.; Wan, Y.; Luo, J. Nanofiltration membrane for bio-separation: Process-oriented materials innovation. *Eng. Life Sci.* **2021**, *21*, 405−416.

(41) Puhlfürß, P.; Voigt, A.; Weber, R.; Morbé, M. Microporous TiO2 membranes with a cut off < 500 Da. *J. Membr. Sci.* **2000**, *174*, 123−133.

(42) Liu, C.; Mao, H.; Zheng, J.; Zhang, S. In situ surface crosslinked tight ultrafiltration membrane prepared by one-step chemical reaction-involved phase inversion process between activated PAEK-COOH and PEI. *J. Membr. Sci.* **2017**, *538*, 58−67.

(43) Chung, Y.; Park, D.; Kim, H.; Nam, S.-E.; Kang, S. Novel method for the facile control of molecular weight cut-off (MWCO) of ceramic membranes. *Water Res.* **2022**, *215*, No. 118268.

(44) Arefi-Oskoui, S.; Khataee, A.; Vatanpour, V. Effect of solvent type on the physicochemical properties and performance of NLDH/PVDF nanocomposite ultrafiltration membranes. *Sep. Purif. Technol.* **2017**, *184*, 97−118.

(45) Du, R.; Gao, B.; Men, J. Microfiltration membrane possessing chelation function and its adsorption and rejection properties towards heavy metal ions. *J. Chem. Technol. Biotechnol.* **2019**, *94*, 1441−1450.

(46) Bal-Demirci, T. Synthesis, spectral characterization of the zinc(II) mixed-ligand complexes of N(4)-allyl thiosemicarbazones and N,N,N′,N′-tetramethylethylenediamine, and crystal structure of the novel [ZnL2(tmen)] compound. *Polyhedron* **2008**, *27*, 440−446.

(47) Matesanz, A. I.; Leitao, I.; Souza, P. Palladium(II) and platinum(II) bis(thiosemicarbazone) complexes of the 2,6-diacetyl-pyridine series with high cytotoxic activity in cisplatin resistant A2780cisR tumor cells and reduced toxicity. *J. Inorg. Biochem.* **2013**, *125*, 26−31.

(48) Dehno Khalaji, A.; Shahsavani, E.; Feizi, N.; Kucerakova, M.; Dusek, M.; Mazandarani, R. Silver(I) thiosemicarbazone complex [Ag(catsc)(PPh3)2]NO3: Synthesis, characterization, crystal structure, and antibacterial study. *C. R. Chim.* **2017**, *20*, 534−539.

(49) Tian, T.; Hu, R.; Tang, B. Z. Room Temperature One-Step Conversion from Elemental Sulfur to Functional Polythioureas through Catalyst-Free Multicomponent Polymerizations. *J. Am. Chem. Soc.* **2018**, *140*, 6156−6163.

(50) Alomar, K.; Landreau, A.; Allain, M.; Bouet, G.; Larcher, G. Synthesis, structure and antifungal activity of thiophene-2,3-dicarboxaldehyde bis(thiosemicarbazone) and nickel(II), copper(II) and cadmium(II) complexes: Unsymmetrical coordination mode of nickel complex. *J. Inorg. Biochem.* **2013**, *126*, 76−83.

(51) Akgül, M.; Karabakan, A.; Acar, O.; Yürüm, Y. Removal of silver (I) from aqueous solutions with clinoptilolite. *Microporous Mesoporous Mater.* **2006**, *94*, 99−104.

(52) Liu, P.; Sehaqui, H.; Tingaut, P.; Wichser, A.; Oksman, K.; Mathew, A. P. Cellulose and chitin nanomaterials for capturing silver ions (Ag+) from water via surface adsorption. *Cellulose* **2014**, *21*, 449−461.

(53) Zhang, M.; Helleur, R.; Zhang, Y. Ion-imprinted chitosan gel beads for selective adsorption of Ag+ from aqueous solutions. *Carbohydr. Polym.* **2015**, *130*, 206−212.

(54) Zhang, Y.; Wang, K.; Duan, G.; Chen, Y.; Liu, K.; Hou, H. Efficient removal of high- or low-concentration copper ions using diethylenetriamine-grafted electrospun polyacrylonitrile fibers. *New J. Chem.* **2023**, *47*, 5639−5649.

(55) Yang, W.; Wang, Y.; Wang, Q.; Wu, J.; Duan, G.; Xu, W.; Jian, S. Magnetically separable and recyclable Fe3O4@PDA covalent grafted by l-cysteine core-shell nanoparticles toward efficient removal of Pb2+. *Vacuum* **2021**, *189*, No. 110229.

(56) Song, J.; Yang, W.; Han, X.; Jiang, S.; Zhang, C.; Pan, W.; Jian, S.; Hu, J. Performance of Rod-Shaped Ce Metal−Organic Frameworks for Defluoridation. *Molecules* **2023**, *28*, No. 3492.

🕮 Recommended by ACS